



Published in final edited form as:

*Biochemistry*. 2009 September 29; 48(38): 9122–9131. doi:10.1021/bi900675v.

## Effects of Putative Catalytic Base Mutation E211Q on ABCG2-Mediated Methotrexate Transport

Yue-xian Hou<sup>1</sup>, Chang-Zhong Li<sup>1</sup>, Kanagaraj Palaniyandi<sup>1</sup>, Paul M. Magtibay<sup>1</sup>, Laszlo Homolya<sup>2</sup>, Balazs Sarkadi<sup>2</sup>, and Xiu-bao Chang

<sup>1</sup>Department of Biochemistry and Molecular Biology, Mayo Clinic College of Medicine, 13400 East Shea Blvd, Scottsdale, Arizona, U.S.A., 85259

<sup>2</sup>Membrane Biology, Hungarian Academy of Sciences, Dioszegi 64, 1113 Budapest, Hungary

### Abstract

ABCG2 is a half ATP binding cassette (ABC) drug transporter that consists of a nucleotide binding domain (NBD) followed by a trans-membrane domain. This half ABC transporter is thought to form a homodimer in the plasma membrane where it transports anticancer drugs across the biological membranes in an ATP-dependent manner. Substitution of the putative catalytic residue E211 with a non-acidic amino acid glutamine (E211Q) completely abolished its ATPase activity and ATP-dependent methotrexate transport, suggesting that ATP hydrolysis is required for the ATP-dependent solute transport. However, whether one ATP hydrolysis or two ATP hydrolyses in the homodimer of ABCG2 with NBD·ATP·ATP·NBD sandwich structure is/are required for the ATP-dependent solute transport is not known yet. To address this question, we have made an YFP/ABCG2 fusion protein and expressed this 99 kDa fusion protein alone or along with the 70 kDa E211Q-mutated ABCG2 in BHK cells. Although membrane vesicles prepared from BHK cells expressing YFP/ABCG2 exert higher ATPase activity than that of wt ABCG2, the dATP-dependent methotrexate transport activities of these two proteins are the same. Interestingly, membrane vesicles prepared from BHK cells expressing both YFP/ABCG2 and E211Q-mutated ABCG2 (with a ratio of 1:1) form homodimers and heterodimer and exert 55% of wtABCG2 ATPase activity that can be further enhanced by anticancer drugs, suggesting that the wt NBD in the heterodimer of YFP/ABCG2 and E211Q may be able to hydrolyze ATP. Furthermore, the membrane vesicles containing both YFP/ABCG2 and E211Q exert ~ 79% of wtABCG2-mediated methotrexate transport activity, implying that the heterodimer harboring YFP/ABCG2 and E211Q may be able to transport the anticancer drug methotrexate across the biological membranes.

### Keywords

ABCG2; NBD; homodimers and heterodimer; ATPase; MTX; ATP-dependent MTX transport

Development of multidrug resistance (MDR) in cancer cells leads to chemotherapeutic treatment failure. Over-expression of some of the ATP binding cassette (ABC) drug transporters, such as P-glycoprotein (P-gp or ABCB1), multidrug resistance-associated protein (MRP1 or ABCC1) and/or breast cancer resistance protein (BCRP, ABCP, MXR or ABCG2), confers “acquired” MDR (1-7). These drug transporters couple ATP binding/hydrolysis to anticancer drug transport. Thus, understanding the molecular mechanisms of the ATP-

\*Corresponding Author Footnote: Department of Biochemistry and Molecular Biology, Mayo Clinic College of Medicine, 13400 East Shea Blvd, Scottsdale, Arizona, U.S.A., 85259, Tel. 480-301-6206; Fax 480-301-7017. xbchang@mayo.edu.

dependent anticancer drug transport by these transporters may provide a basis for overcoming the MDR caused by over-expression of these proteins.

Most functional eukaryotic ABC transporters, such as ABCB1 (5,8) or ABCC1 (2,9,10), consist of two nucleotide binding domains (NBD) and two transmembrane domains (TMD). However, ABCG2 is a much smaller protein than either ABCB1 or ABCC1 and considered as a half ABC transporter consisting of an N-terminal NBD and a C-terminal TMD (3,4,7). This half ABC transporter was thought to form a homo-dimer in the plasma membrane (11-14). Thus, the functional ABCG2 contains two identical NBDs.

Since all the functional ABC transporters contain two NBDs (2,5,11-15), an important question to be asked is why these ABC transporters require two NBDs. Structure analyses of several prokaryotic ABC transporter NBDs clearly answered this question. The two NBDs form a dimer in which the two ATP molecules are each sandwiched between the Walker A motif from one NBD and the LSGGQ ABC signature motif from another (16-22). In addition, many other residues, such as the residues from the Walker B motif, A-loop, Q-loop, H-loop and D-loop (16,17,19,20,22-39), contribute to the Mg-ATP binding. Upon Mg-ATP binding to form NBD-ATP-ATP-NBD sandwich structure, the acidic amino acid directly adjacent to the aspartic acid in Walker B motif or putative catalytic base (16) will activate water molecule to attack the bound Mg-ATP.

Since ABCG2 contains two identical NBDs, whether the two ATP molecules bound in the NBD-ATP-ATP-NBD sandwich structure will be hydrolyzed simultaneously or not is an interesting question. To address this question, we have mutated the putative catalytic base E211 to Q and expressed this mutant in BHK cells. Interestingly, E211Q mutation (in homodimer) completely abolished its ATPase activity and ATP-dependent anticancer drug transport, whereas co-expression of this mutant with YFP/ABCG2 fusion protein may form a functional heterodimer with altered kinetic parameters.

## Experimental Procedures

### Materials

EDTA, EGTA, ATP, dATP, sucrose, ouabain, sodium azide and other chemicals were purchased from Sigma. Methotrexate (MTX), manufactured by Lederle Parenterals, was derived from Mayo Clinic Arizona Pharmacy. [3',5',7-<sup>3</sup>H]-MTX was from Amersham. ABCG2 monoclonal antibody BXP-21 was from ID Labs. Cellulose membrane filters and ammonium molybdate were from Fisher Scientific.

### Generation of constructs

Wild-type BCRP cDNA was derived from Dr. Douglas D. Ross (4) and amplified by using the forward primer containing the Kozak sequence (40) ACC ATG G with an initiation ATG codon followed by a T242G mutation (or S2A mutation) and the reverse primer containing CAT CAC CAT CAC CAT CAC (8 histidine codons at the C-terminus of BCRP) followed by a stop codon TAG. The polymerase chain reaction (PCR) amplified BCRP/his cDNA was inserted into pNUT expression vector (41-43), named as pNUT/BCRP/his. In order to remove the 8 histidine residues at the C-terminus of BCRP/his, a stop codon TAG was introduced into pNUT/BCRP/his by using the forward/reverse primers and the QuikChange site directed mutagenesis kit from Stratagene (44), named as pNUT/ABCG2. The putative catalytic residue E211 was mutated to Q in pNUT/ABCG2, named as pNUT/ABCG2/E211Q. In order to distinguish the wt ABCG2 from the E211Q-mutated protein, the full length yellow fluorescent protein (YFP) cDNA (238 amino acids) with the SGLRSRAAANT (11 amino acids) linker (45), amplified by PCR from the plasmid DNA containing YFP cDNA (46), was inserted into

the N-terminus of pNUT/ABCG2, named as pNUT/YFP/ABCG2. All the fragments amplified by PCR were confirmed by DNA sequencing.

### Cell Culture and Cell lines expressing ABCG2

Baby hamster kidney (BHK) cells were cultured in DMEM/F-12 media supplemented with 5% fetal bovine serum at 37 °C in 5% CO<sub>2</sub>. Subconfluent cells were transfected with pNUT/ABCG2 plasmid DNA in the presence of 20 mM HEPES (pH 7.05), 137 mM NaCl, 5 mM KCl, 0.7 mM Na<sub>2</sub>HPO<sub>4</sub>, 6 mM dextrose and 125 mM CaCl<sub>2</sub> (43). Surviving individual colonies in media containing 250 μM MTX, based on the presence of MTX-resistant DHFR mutant in pNUT expression vector (41), were picked and amplified. Cells for membrane vesicle preparation were grown in DMEM/F12 media containing 5% fetal bovine serum and 100 μM MTX in roller bottles (on a roller machine from BELLCO).

### Detection of ABCG2 protein

Western blot was performed according to the method described previously (44). BXP-21 monoclonal antibody was used to identify the ABCG2 protein expressed in BHK cells. The secondary antibody used was anti-mouse Ig conjugated with horse radish peroxidase. Chemiluminescent film detection was performed according to the manufacturer's recommendations (Pierce).

### Endoglycosidase H treatment of protein

The core-glycosylated oligosaccharides were removed by digestion with endoglycosidase H. Cells were lysed with 2% SDS and sonicated for 20 pulses to break the genomic DNA. 10 μg of the cell lysates were digested overnight at 37 °C with 200 units (New England BioLabs) of endoglycosidase H in 200 μl of solution containing 50 mM sodium acetate buffer (pH 5.3), 0.5% NP-40, 1% β-mercaptoethanol, 0.2% SDS, 10 μg bovine serum albumin and 1 × protease inhibitors (47). Following digestion, 800 μl of cold ethanol was added to precipitate the proteins. The pellets were collected by centrifugation at 4 °C for 15 minutes. The proteins were resolved by SDS-PAGE (7%), electroblotted to a nitrocellulose membrane and probed with BXP-21 mAb against human ABCG2.

### Membrane vesicle preparations

ABCG2-containing membrane vesicles were prepared according to the procedure described previously (44). The membrane vesicle pellet was re-suspended in a solution containing 10 mM Tris-HCl (pH 7.5), 250 mM sucrose and 1 × protease inhibitors (2 μg/ml aprotinin, 121 μg/ml benzamidin, 3.5 μg/ml E64, 1 μg/ml leupeptin and 50 μg/ml Pefabloc). After passage through a Liposofast™ vesicle extruder (Avestin, Ottawa, Canada) aliquots of the membrane vesicles were stored in -80 °C.

### Membrane vesicle transport

ATP-dependent transport of <sup>3</sup>H-labeled MTX into the membrane vesicles was assayed by a rapid filtration technique (48,49). The assays were carried out in a 30 μl solution (in triplicate) containing 3 μg of membrane proteins, 50 mM Tris-HCl (pH 7.5), 250 mM sucrose, 10 mM MgCl<sub>2</sub>, 2 mM MTX (90 nCi of <sup>3</sup>H-labeled MTX) and 4 mM ATP or 4 mM dATP (as indicated in the Figure legends). After incubation at 37 °C for 7.5 min, the samples were brought back to ice and diluted with 1 ml of ice-cold 1 × transport buffer (50 mM Tris-HCl, pH 7.5, 250 mM sucrose and 10 mM MgCl<sub>2</sub>) and trapped on nitrocellulose membranes (0.2 μm) that had been equilibrated with 1 × transport buffer. The filter was then washed with 10 ml of ice-cold 1 × transport buffer, air-dried and placed in a 10 ml of biodegradable counting scintillant (Amersham Pharmacia Biotech). The radioactivity bound to the nitrocellulose membrane was determined by liquid scintillation counting (Beckman LS 6000SC).

### ATPase assay

The ATPase activity of ABCG2 protein was determined according to the method published previously (50). Briefly, 2  $\mu$ g of membrane proteins in 50  $\mu$ l of reaction buffer containing 50 mM KCl, 2.5 mM MgSO<sub>4</sub>, 3 mM dithiothreitol, 25 mM Tris-HCl (pH 7.0), 4 mM ATP, 0.5 mM EGTA (to inhibit Ca-ATPases), 2 mM ouabain [to inhibit the (Na+K)-ATPases] and 3 mM azide (to inhibit mitochondrial ATPases) in 96-well plate (in triplicate) were incubated at 37 °C for 30 minutes and terminated by addition of 200  $\mu$ l ice-cold stopping solution [0.2% (w/v) ammonium molybdate; 1.3% (v/v) sulfuric acid; 0.9% (w/v) SDS; 2.3% (w/v) trichloroacetic acid; and freshly prepared ascorbic acid, 1% (w/v)] to each well. After 30 min incubation at room temperature, the released inorganic phosphate was quantified colorimetrically in a microplate reader (Bio-Tek Instruments, VT, USA) at 650 nm. Phosphate buffer (pH7.4, from 16 to 512  $\mu$ M) was used to establish the standard curve. Background in 4 mM ATP and BHK membrane vesicle control experiments were obtained in parallel and subtracted from the measurements (described in Figure legends).

### Statistical analysis

The results in Figures 2, 3, 4 and 5 were presented as means  $\pm$  SD. The two-tailed P values were calculated based on the unpaired t test from GraphPad Software Quick Calcs. By conventional criteria, if P value is less than 0.05, the difference between two samples is considered to be statistically significant.

## Results

### Substitution of the putative catalytic residue E211 with a non-acidic amino acid Q abrogated its ATP-dependent MTX transport

In order to test whether substitution of the ABCG2 putative catalytic base E211 with a glutamine residue (E211Q) is able to transport MTX across biological membranes, membrane vesicles have been prepared from the BHK cells expressing either wt or E211Q-mutated ABCG2. The results in Figure 1A indicate that the amount of wtABCG2 is similar to that of E211Q, whereas there is no detectable amount of ABCG2 in membrane vesicles prepared from the parental or cystic fibrosis transmembrane-conductance regulator (CFTR or ABCC7) cDNA-transfected BHK cells. Membrane vesicles prepared from the wtABCG2-transfected BHK cells were able to transport MTX across the biological membranes (Fig. 1B) and the amounts of MTX transported into membrane vesicles, in the presence of 4 mM dATP, reach plateau after 7.5 minutes incubation at 37 °C (Fig. 1C). Although the amount of E211Q-mutated ABCG2 is similar to that of wtABCG2, E211Q mutated ABCG2, similar to CFTR and BHK membrane vesicles, was unable to transport MTX across the biological membranes (Fig. 1B), suggesting that substitution of the putative catalytic base of ABCG2 with a non-acidic glutamine residue may completely abolish its ATPase activity.

It has been reported that ABCG2 forms inter- and intra-molecular disulfide bonds (45,51-53). We have asked a question of whether the disulfide bond formation in ABCG2 protein would affect ATP-dependent anticancer drug transport or not. The results in Figure 1D clearly indicate that the reducing agents, such as  $\beta$ -mercaptoethanol or dithiothreitol, significantly (p values are less than 0.05) enhanced the ATP- or dATP-dependent MTX transport activities.

### The heterodimer of YFP/ABCG2 and E211Q may be able to transport MTX across the biological membranes

Since E211Q-mutated ABCG2 completely abrogated its ATP-dependent MTX transport activity (Fig. 1B), we had asked a question of whether the heterodimer of wt and E211Q-mutated ABCG2 was able to transport MTX across the biological membranes or not. However,

because the wt ABCG2 and the E211Q-mutated ABCG2 run to the same position in SDS-PAGE (as shown in Fig. 1A), there was no way to distinguish these two proteins if they were co-expressed in BHK cells. Thus, we decided to insert YFP protein, with the SGLRSRAAANT linker (45), into the N-terminus of ABCG2. When this fusion protein was expressed in BHK cells at 37 °C, majority of the protein were resistant to the endoglycosidase H digestion (Fig. 2A), indicating that insertion of the YFP protein to the N-terminus of ABCG2 did not significantly affect the protein folding. The complex-glycosylated YFP/ABCG2 has an apparent molecular weight of  $\sim 99 \pm 3$  kDa (Fig. 2B, n = 16), which is significantly larger than its un-modified wt or E211Q-mutated ABCG2, with an apparent molecular weight of  $\sim 70 \pm 2$  kDa (Fig. 2B, n = 24). Due to the mobility difference between YFP/ABCG2 and E211Q-mutated ABCG2, these two proteins co-expressed in BHK cells can be separated very well (Fig. 2B). Furthermore, the ratio between the complex-glycosylated YFP/ABCG2 and E211Q, probed with the same ABCG2-specific mAb BXP-21, can be accurately determined. Thus, YFP/ABCG2 was co-expressed with E211Q (with plasmid DNA ratios of 2:8; 4:6; 5:5; 6:4; or 8:2) in BHK cells. Individual colonies were picked and analyzed by western blots. Colonies derived from the transfections with ratios of 4:6, 5:5 or 6:4 yielded similar amounts of YFP/ABCG2 and E211Q. Membrane vesicles were prepared from the colonies with similar amounts of YFP/ABCG2 and E211Q and analyzed by western blots. Membrane vesicles containing the same amounts of YFP/ABCG2 and E211Q (with a ratio of 1:1 as shown in Fig. 2B) were used to do further analysis.

When the membrane vesicles were separated in SDS-PAGE in the absence of reducing agent DTT, wtABCG2 or E211Q monomer ( $70 \pm 2$  kDa) and homodimer ( $149 \pm 0$  kDa) and YFP/ABCG2 monomer ( $99 \pm 3$  kDa) and homodimer ( $220 \pm 1$  kDa) and heterodimer of YFP/ABCG2 and E211Q ( $188 \pm 0$  kDa) were clearly detected (Fig. 2C). Interestingly, in the 4-10% gradient gel (Fig. 2C), the ratio of E211Q and YFP/ABCG2 is approximately 1 :  $1.1 \pm 0.2$ , implying that similar amounts of E211Q and YFP/ABCG2 form either homodimer or heterodimer. The ratios between the homodimers and heterodimer further confirm this conclusion, i.e., homodimer of YFP/ABCG2 ( $30.0 \pm 3.2\%$ , n=25), homodimer of E211Q ( $28.2 \pm 3.8\%$ , n=25) and the heterodimer of YFP/ABCG2 and E211Q ( $41.8 \pm 3.6\%$ , n=25). Thus, regardless of whether the intermolecular disulfide bond is formed *in vivo* or *in vitro*, the heterodimer of YFP/ABCG2 and E211Q does exist in the plasma membranes of the BHK cells co-transfected with YFP/ABCG2 and E211Q-mutated ABCG2.

We then questioned whether the ATP bound to the heterodimer can be hydrolyzed or not. In order to address this question, the same amount of ABCG2 protein should be used to do the ATPase assay. Since all the samples were probed with the same ABCG2 mAb BXP-21 (as shown in Fig. 2B), the relative intensities of the bands were used to calculate the relative ratios of these proteins. The ratio between YFP/ABCG2 and E211Q is  $\sim 1.0375 \pm 0.0303$  (n = 4), indicating that the amount of YFP/ABCG2 protein in the membrane vesicles containing both YFP/ABCG2 and E211Q is not significantly different from that of E211Q-mutated ABCG2. The ratios between different samples and wt ABCG2 are:  $2.3821 \pm 0.3762$  (YFP/ABCG2 + E211Q, including both YFP/ABCG2 and E211Q bands, versus wtABCG2, n = 4);  $0.9431 \pm 0.1758$  (E211Q versus wtABCG2, n = 4);  $1.2454 \pm 0.1878$  (YFP/ABCG2 versus wtABCG2, n=4). The results in Figure 2D indicate that wtABCG2 is able to hydrolyze ATP, with a velocity of  $\sim 40$  nmol·mg<sup>-1</sup>·min<sup>-1</sup>, whereas YFP/ABCG2, after adjusted with BHK membrane vesicles to have the same amount of ABCG2 protein, is moderately more active than that of wtABCG2. However, E211Q alone is unable to hydrolyze ATP, indicating that substitution of the putative catalytic residue E211 with a glutamine residue completely abolished its ATPase activity. Co-expression of YFP/ABCG2 with E211Q yielded  $\sim 55\%$  of wtABCG2 ATPase activity (Fig. 2D), making difficult to make any conclusion from this result. However, in considering the results published by Henriksen et al., i.e., coexpression of wt ABCG2 with K86M-mutated ABCG2 exerted  $\sim 50\%$  of wt ABCG2 ATPase activity (54), the above result might be

interpreted as that one of the two ATPs bound to the heterodimer of YFP/ABCG2 and E211Q could be hydrolyzed. If that is the case, we then questioned whether one ATP hydrolysis in this heterodimer will support the ATP-dependent anticancer drug transport or not. The fact that the dATP-dependent MTX transport activity of YFP/ABCG2 is almost the same as wtABCG2 (Fig. 2E and Table 1) indicates that insertion of YFP protein into the N-terminus of ABCG2 does not significantly affect the protein function. In contrast, E211Q alone is unable to transport MTX across the biological membranes (Fig. 2E). However, co-expression of YFP/ABCG2 with E211Q (with a ratio of 1:1), after adjusted with BHK membrane vesicles to have similar amount of ABCG2 in YFP/ABCG2 + E211Q as in wtABCG2, yielded approximately 79% of wtABCG2 transport activity (Fig. 2E and Table 1), suggesting that the heterodimer of YFP/ABCG2 and E211Q may be able to transport MTX into the membrane vesicles.

### Heterodimer formation of YFP/ABCG2 and E211Q altered the kinetic parameters of nucleotide-dependent MTX transport

If the heterodimer of YFP/ABCG2 and E211Q is able to transport MTX into the membrane vesicles, we expect that the kinetic parameters of nucleotide-dependent MTX transport may be changed. In order to address this question, we have to prove that insertion of the YFP protein into the N-terminus of ABCG2 does not have a significant effect on the kinetic parameters of nucleotide-dependent MTX transport. ATP- (Fig. 3A) and dATP-dependent (Fig. 3B) MTX transport by YFP/ABCG2 exert typical Michaelis-Menten curves. These yield  $K_m$  and  $V_{max}$  values of  $455 \pm 19 \mu\text{M}$  ATP,  $274 \pm 31 \mu\text{M}$  dATP,  $161 \pm 21 \text{ nmol}\cdot\text{mg}^{-1}\cdot\text{min}^{-1}$  and  $149 \pm 10 \text{ nmol}\cdot\text{mg}^{-1}\cdot\text{min}^{-1}$  (Table 2), implying that the protein has higher affinity for dATP than that of ATP. These values are not significantly different from the kinetic parameters of wtABCG2 (Table 2, with  $p$  values much higher than 0.1). In contrast, the ATP- (Fig. 3C) and dATP-dependent (Fig. 3D) MTX transport by membrane vesicles containing both YFP/ABCG2 and E211Q exerted two (mixed) Michaelis-Menten curves: one yields lower  $K_m$  and  $V_{max}$  values and another, higher  $K_m$  and  $V_{max}$  values (due to overlap between these two curves, the  $K_m$  and  $V_{max}$  values cannot be accurately determined). The results were interpreted as that the MTX transported into membrane vesicles at lower concentrations of nucleotides was catalyzed by the homodimer of YFP/ABCG2, whereas the one transported into membrane vesicles at higher concentrations of nucleotides was catalyzed by both homodimer of YFP/ABCG2 and heterodimer of YFP/ABCG2 and E211Q.

### Anticancer drugs enhanced the ABCG2 ATPase activity

Since ABCG2 transports anticancer drugs across the biological membrane in an ATP dependent manner, anticancer drugs may enhance the ATPase activity of ABCG2. The results in Figure 4 indicated that the basal ATPase activity ( $\sim 40 \text{ nmol}\cdot\text{mg}^{-1}\cdot\text{min}^{-1}$ ) of membrane vesicles derived from BHK cell is the same as the one derived from BHK/E211Q cell, indicating that E211Q protein does not have ability to hydrolyze ATP. These results also indicated that EGTA, ouabain and sodium azide did not completely inhibit all the ATPases in BHK membrane vesicles. The basal ATPase activities of membrane vesicles containing wtABCG2 ( $\sim 80 \text{ nmol}\cdot\text{mg}^{-1}\cdot\text{min}^{-1}$  without subtracting the ATPase activity contributed by BHK membrane proteins), YFP/ABCG2 ( $\sim 105 \text{ nmol}\cdot\text{mg}^{-1}\cdot\text{min}^{-1}$ ) or YFP/ABCG2 + E211Q ( $\sim 76 \text{ nmol}\cdot\text{mg}^{-1}\cdot\text{min}^{-1}$ ) were significantly higher than that of BHK or E211Q membrane vesicles, indicating that wtABCG2, YFP/ABCG2 or YFP/ABCG2 + E211Q can hydrolyze ATP in the absence of their substrate. Furthermore, the basal ATPase activities of either BHK membrane proteins or E211Q cannot be enhanced by anticancer drugs, such as daunomycin (Fig. 4A), methotrexate (Fig. 4B) or tamoxifen (Fig. 4C), whereas the ATPase activities wtABCG2, YFP/ABCG2 or YFP/ABCG2 + E211Q are either significantly or moderately enhanced by anticancer drugs, such as daunomycin (Fig. 4A), methotrexate (Fig. 4B) or tamoxifen (Fig. 4C), suggesting that only the ATPase activity contributed by ABCG2 protein can be enhanced by anticancer drugs.

## Discussion

ABCG2 homodimer transports the anticancer drug MTX across biological membranes in an ATP dependent manner (55,56) and the ATPase activity of this protein in membrane vesicles is readily detectable. Substitution of the putative catalytic E211 residue with a non-charged amino acid glutamine (E211Q) completely abolished its ATPase activity (Fig. 2 and 4), suggesting that the acidic amino acid E211 plays a very important role in ATP hydrolysis. E211Q mutation also completely abolished the dATP-dependent MTX transport (Fig. 1 and 2), indicating that ATP hydrolysis is required for facilitating the anticancer drug MTX across the biological membranes. These results are consistent with the corresponding mutations in ABCB1 (57), in ABCC1 (E1455 mutations in NBD2) (58,59) and in bacterial ABC transporters MJ0796 (18) and HisP (27). However, these results are not consistent with the corresponding mutations in NBD1 (the D793 mutations) of ABCC1 (47,58,59). Since ABCG2 forms homodimer *in vivo*, the E211Q mutation actually mutated both putative catalytic bases in the two NBDs of the homodimer of this protein. Therefore these results cannot answer the question of whether one ATP hydrolysis or two ATP hydrolyses in the NBD·ATP·ATP·NBD sandwich structure is or are required for the ATP-dependent solute transport by ABCG2.

In order to address the question mentioned above, we have made an YFP/ABCG2 fusion protein (with an apparent molecular weight of 99 kDa) so that it can be clearly distinguished from the E211Q-mutated ABCG2 (with an apparent molecular weight of 70 kDa). Similar to GFP-G2 (45), insertion of YFP to the N-terminus of ABCG2 did not have a significant effect on the protein folding and processing (Fig. 2A). This complex-glycosylated fusion protein is able to hydrolyze ATP (Fig. 2D) and its ATPase activity can be significantly enhanced by anticancer drugs, such as daunomycin (Fig. 4A), MTX (Fig. 4B) or tamoxifen (Fig. 4C). These data are in harmony with the previous published results (60-63). Furthermore, this YFP/ABCG2 fusion protein did not significantly alter the kinetic parameters of this transporter (Table 2). Thus, if the YFP/ABCG2 fusion protein can form heterodimer with E211Q mutated ABCG2, this heterodimer may be used to test whether the ATP bound in the NBD·ATP·ATP·NBD-E211Q sandwich structure can be hydrolyzed or not. Indeed, when YFP/ABCG2 was co-expressed with E211Q mutated ABCG2 in BHK cells, approximately 42% of them form heterodimer in the BHK plasma membranes (Fig. 2C). Although E211Q mutation completely abolished its ATPase activity (Fig. 2D and 4), co-expression of YFP/ABCG2 with E211Q mutated ABCG2 exerted ~ 55% of wtABCG2 ATPase activity (Fig. 2D). This is consistent with Henriksen's result that coexpression of wt ABCG2 with K86M-mutated ABCG2 exerted ~ 50% of wt ABCG2 ATPase activity (54). This ATPase activity, regardless of whether it is contributed by wt NBD from homodimer of YFP/ABCG2 or heterodimer containing YFP/ABCG2 and E211Q-mutated ABCG2, can be further stimulated by anticancer drugs, such as daunomycin (Fig. 4A), MTX (Fig. 4B) or tamoxifen (Fig. 4C), implying that one of the two ATPs bound in the NBD·ATP·ATP·NBD-E211Q sandwich structure could be hydrolyzed. Of course, this conclusion should be further confirmed by using covalently-linked dimers (64), such as wtABCG2-wtABCG2, E211Q-E211Q and wtABCG2-E211Q (which is our ongoing project).

The above conclusion implies that one of the two ATPs bound in the NBD·ATP·ATP·NBD-E211Q sandwich structure could be hydrolyzed by wtNBD. If that is the case, the heterodimer of YFP/ABCG2 and E211Q may be used to address the question of whether one ATP hydrolysis or two ATP hydrolyses in the NBD·ATP·ATP·NBD sandwich structure is or are required for the ATP-dependent solute transport by ABCG2. As mentioned in previous paragraph that insertion of the YFP protein into the N-terminus of ABCG2 did not significantly alter the kinetic parameters of this transporter (Table 2). However, substitution of the putative catalytic base E211 with a glutamine residue completely abolished its ATP-dependent MTX transport (Fig. 1B, 2E and Table 1). Interestingly, membrane vesicles containing the same amount of E211Q and YFP/ABCG2 exerted ~ 79% of wtABCG2 (Table 1), which is very close to the

theoretical value of 75% of wtABCG2. This 79% transport activity is not caused by the MTX selection to enhance the endogenous ABCG2 expression because the MTX selection was based on the tolerance of the dihydrofolate reductase (DHFR) mutant harbored in pNUT expression vector (41). Furthermore, membrane vesicles prepared from BHK/CFTR (Fig. 1) and BHK/E211Q (Fig. 1 and 2), which were generated under the same selection procedures as YFP/ABCG2 + E211Q, were unable to transport MTX across the biological membranes. These results suggest that the heterodimer containing YFP/ABCG2 and E211Q-mutated ABCG2 is able to transport the bound MTX into the membrane vesicles, strikingly contrasting the conclusions derived from K86M- or D210N-mutated ABCG2 (11,54,64). Since human ABCG2 has a trend to form tetramer (53), there is a possibility that the wtNBD from one heterodimer might contact with the wtNBD in another and form a functional hetero-tetramer. Kinetic analyses of the membrane vesicles containing both YFP/ABCG2 and E211Q mutated ABCG2 (Fig. 3C and 3D) indicate that there might be two populations of membrane vesicles: one population has lower  $K_m$  and  $V_{max}$  values and another, higher  $K_m$  and  $V_{max}$  values. In view of the conclusion made by McDevitt et al. (65), i.e., ATP binding to NBD of ABCG2 induces conformational changes that result in shifting the bound anticancer drug from high to low affinity site, we interpreted these results as that ATP binding to the heterodimer of E211Q and YFP/ABCG2 might induce proper conformational changes that brought the bound MTX from high to low affinity site. One ATP hydrolysis in the NBD-ATP-ATP-NBD-E211Q sandwich structure, catalyzed by the wtNBD, may facilitate the release of both nucleotides bound in this sandwich structure and bring the molecule back to its original conformation so that the protein can start a new cycle of ATP-dependent solute transport. If this is the case, the higher  $K_m$  value of a population, possibly the heterodimer of YFP/ABCG2 and E211Q, implies that higher concentration of nucleotide is required to form the NBD-ATP-ATP-NBD-E211Q sandwich structure. If K86M- or D210N-mutated ABCG2 had higher effects on ATP binding than E211Q, much higher concentration of ATP may be required to form the NBD-ATP-ATP-NBD-K86M or NBD-ATP-ATP-NBD-D210N sandwich structure. This interpretation is consistent with previous findings, i.e., mutations having limited effects on ATP binding, such as MRP1/D793 mutations (59), may retain their ability to transport the bound substrate across the biological membranes, whereas the mutations having significant effects on ATP binding, such as MRP1/K684, MRP1/K1333, MRP1/D792 and MRP1/D1454 mutations (44,47,66-69), may dramatically lose their abilities to transport the bound substrate across the biological membranes. Thus, ATP binding to the two NBDs plays a crucial role for the formation of NBD-ATP-ATP-NBD sandwich structure and for the ATP-dependent solute transport by ABC transporters.

## Acknowledgments

We'd like to take this opportunity to thank Dr. Douglas D. Ross for providing human ABCG2 cDNA. We appreciate Irene Beauvais for helping us in preparing the manuscript and Marv Ruona for his expertise in preparing the figures.

This work was supported by a grant from the National Cancer Institute (CA89078, X.B.C.).

## References

1. Juliano RL, Ling V. A surface glycoprotein modulating drug permeability in Chinese hamster ovary cell mutants. *Biochim Biophys Acta* 1976;455:152–162. [PubMed: 990323]
2. Cole SP, Bhardwaj G, Gerlach JH, Mackie JE, Grant CE, Almquist KC, Stewart AJ, Kurz EU, Duncan AM, Deeley RG. Overexpression of a transporter gene in a multidrug-resistant human lung cancer cell line [see comments]. *Science* 1992;258:1650–1654. [PubMed: 1360704]
3. Allikmets R, Schriml LM, Hutchinson A, Romano-Spica V, Dean M. A human placenta-specific ATP-binding cassette gene (ABCP) on chromosome 4q22 that is involved in multidrug resistance. *Cancer Res* 1998;58:5337–5339. [PubMed: 9850061]



4. Doyle LA, Yang W, Abruzzo LV, Krogmann T, Gao Y, Rishi AK, Ross DD. A multidrug resistance transporter from human MCF-7 breast cancer cells. *Proc Natl Acad Sci U S A* 1998;95:15665–15670. [PubMed: 9861027]
5. Chen CJ, Chin JE, Ueda K, Clark DP, Pastan I, Gottesman MM, Roninson IB. Internal duplication and homology with bacterial transport proteins in the *mdr1* (P-glycoprotein) gene from multidrug-resistant human cells. *Cell* 1986;47:381–389. [PubMed: 2876781]
6. Mirski SE, Gerlach JH, Cole SP. Multidrug resistance in a human small cell lung cancer cell line selected in adriamycin. *Cancer Res* 1987;47:2594–2598. [PubMed: 2436751]
7. Miyake K, Mickley L, Litman T, Zhan Z, Robey R, Cristensen B, Brangi M, Greenberger L, Dean M, Fojo T, Bates SE. Molecular cloning of cDNAs which are highly overexpressed in mitoxantrone-resistant cells: demonstration of homology to ABC transport genes. *Cancer Res* 1999;59:8–13. [PubMed: 9892175]
8. Loo TW, Clarke DM. Mutational analysis of the predicted first transmembrane segment of each homologous half of human P-glycoprotein suggests that they are symmetrically arranged in the membrane. *J Biol Chem* 1996;271:15414–15419. [PubMed: 8663176]
9. Hipfner DR, Almquist KC, Leslie EM, Gerlach JH, Grant CE, Deeley RG, Cole SP. Membrane topology of the multidrug resistance protein (MRP). A study of glycosylation-site mutants reveals an extracytosolic NH<sub>2</sub> terminus. *J Biol Chem* 1997;272:23623–23630. [PubMed: 9295302]
10. Bakos E, Hegedus T, Hollo Z, Welker E, Tusnady GE, Zaman GJ, Flens MJ, Varadi A, Sarkadi B. Membrane topology and glycosylation of the human multidrug resistance-associated protein. *J Biol Chem* 1996;271:12322–12326. [PubMed: 8647833]
11. Ozvegy C, Varadi A, Sarkadi B. Characterization of drug transport, ATP hydrolysis, and nucleotide trapping by the human ABCG2 multidrug transporter. Modulation of substrate specificity by a point mutation. *J Biol Chem* 2002;277:47980–47990. [PubMed: 12374800]
12. Kage K, Tsukahara S, Sugiyama T, Asada S, Ishikawa E, Tsuruo T, Sugimoto Y. Dominant-negative inhibition of breast cancer resistance protein as drug efflux pump through the inhibition of S-S dependent homodimerization. *Int J Cancer* 2002;97:626–630. [PubMed: 11807788]
13. Litman T, Jensen U, Hansen A, Covitz KM, Zhan Z, Fetsch P, Abati A, Hansen PR, Horn T, Skovsgaard T, Bates SE. Use of peptide antibodies to probe for the mitoxantrone resistance-associated protein MXR/BCRP/ABCP/ABCG2. *Biochim Biophys Acta* 2002;1565:6–16. [PubMed: 12225847]
14. Han B, Zhang JT. Multidrug resistance in cancer chemotherapy and xenobiotic protection mediated by the half ATP-binding cassette transporter ABCG2. *Curr Med Chem Anti-Canc Agents* 2004;4:31–42.
15. Georges E, Tsuruo T, Ling V. Topology of P-glycoprotein as determined by epitope mapping of MRK-16 monoclonal antibody. *J Biol Chem* 1993;268:1792–1798. [PubMed: 7678410]
16. Smith PC, Karpowich N, Millen L, Moody JE, Rosen J, Thomas PJ, Hunt JF. ATP binding to the motor domain from an ABC transporter drives formation of a nucleotide sandwich dimer. *Molecular Cell* 2002;10:139–149. [PubMed: 12150914]
17. Chen J, Lu G, Lin J, Davidson AL, Quioco FA. A tweezers-like motion of the ATP-binding cassette dimer in an ABC transport cycle. *Mol Cell* 2003;12:651–661. [PubMed: 14527411]
18. Moody JE, Millen L, Binns D, Hunt JF, Thomas PJ. Cooperative, ATP-dependent association of the nucleotide binding cassettes during the catalytic cycle of ATP-binding cassette transporters. *J Biol Chem* 2002;277:21111–21114. [PubMed: 11964392]
19. Verdon G, Albers SV, Dijkstra BW, Driessen AJ, Thunnissen AM. Crystal structures of the ATPase subunit of the glucose ABC transporter from *Sulfolobus solfataricus*: nucleotide-free and nucleotide-bound conformations. *J Mol Biol* 2003;330:343–358. [PubMed: 12823973]
20. Locher KP, Lee AT, Rees DC. The *E. coli* BtuCD structure: a framework for ABC transporter architecture and mechanism. *Science* 2002;296:1091–1098. [PubMed: 12004122]
21. Hollenstein K, Frei DC, Locher KP. Structure of an ABC transporter in complex with its binding protein. *Nature* 2007;446:213–216. [PubMed: 17322901]
22. Oldham ML, Khare D, Quioco FA, Davidson AL, Chen J. Crystal structure of a catalytic intermediate of the maltose transporter. *Nature* 2007;450:515–521. [PubMed: 18033289]

23. Gaudet R, Wiley DC. Structure of the ABC ATPase domain of human TAP1, the transporter associated with antigen processing. *Embo J* 2001;20:4964–4972. [PubMed: 11532960]
24. Lu G, Westbrook JM, Davidson AL, Chen J. ATP hydrolysis is required to reset the ATP-binding cassette dimer into the resting-state conformation. *Proc Natl Acad Sci U S A* 2005;102:17969–17974. [PubMed: 16326809]
25. Hopfner KP, Karcher A, Shin DS, Craig L, Arthur LM, Carney JP, Tainer JA. Structural biology of Rad50 ATPase: ATP-driven conformational control in DNA double-strand break repair and the ABC-ATPase superfamily. *Cell* 2000;101:789–800. [PubMed: 10892749]
26. Yuan YR, Blecker S, Martsinkevich O, Millen L, Thomas PJ, Hunt JF. The crystal structure of the MJ0796 ATP-binding cassette. Implications for the structural consequences of ATP hydrolysis in the active site of an ABC transporter. *J Biol Chem* 2001;276:32313–32321. [PubMed: 11402022]
27. Hung LW, Wang IX, Nikaido K, Liu PQ, Ames GF, Kim SH. Crystal structure of the ATP-binding subunit of an ABC transporter. *Nature* 1998;396:703–707. [PubMed: 9872322]
28. Procko E, Ferrin-O'Connell I, Ng SL, Gaudet R. Distinct structural and functional properties of the ATPase sites in an asymmetric ABC transporter. *Mol Cell* 2006;24:51–62. [PubMed: 17018292]
29. de Wet H, McIntosh DB, Conseil G, Baubichon-Cortay H, Krell T, Jault JM, Daskiewicz JB, Barron D, Di Pietro A. Sequence requirements of the ATP-binding site within the C-terminal nucleotide-binding domain of mouse P-glycoprotein: structure-activity relationships for flavonoid binding. *Biochemistry* 2001;40:10382–10391. [PubMed: 11513617]
30. Ramaen O, Leulliot N, Sizun C, Ulryck N, Pamard O, Lallemand JY, Tilbeurgh H, Jacquet E. Structure of the human multidrug resistance protein 1 nucleotide binding domain 1 bound to Mg<sup>2+</sup>/ATP reveals a non-productive catalytic site. *J Mol Biol* 2006;359:940–949. [PubMed: 16697012]
31. Zaitseva J, Jenewein S, Jumpertz T, Holland IB, Schmitt L. H662 is the linchpin of ATP hydrolysis in the nucleotide-binding domain of the ABC transporter HlyB. *Embo J* 2005;24:1901–1910. [PubMed: 15889153]
32. Lewis HA, Buchanan SG, Burley SK, Connors K, Dickey M, Dorwart M, Fowler R, Gao X, Guggino WB, Hendrickson WA, Hunt JF, Kearins MC, Lorimer D, Maloney PC, Post KW, Rajashankar KR, Rutter ME, Sauder JM, Shriver S, Thibodeau PH, Thomas PJ, Zhang M, Zhao X, Emtage S. Structure of nucleotide-binding domain 1 of the cystic fibrosis transmembrane conductance regulator. *Embo J* 2004;23:282–293. [PubMed: 14685259]
33. Karpowich N, Martsinkevich O, Millen L, Yuan YR, Dai PL, MacVey K, Thomas PJ, Hunt JF. Crystal structures of the MJ1267 ATP binding cassette reveal an induced-fit effect at the ATPase active site of an ABC transporter. *Structure (Camb)* 2001;9:571–586. [PubMed: 11470432]
34. Diederichs K, Diez J, Greller G, Muller C, Breed J, Schnell C, Vonnrhein C, Boos W, Welte W. Crystal structure of MalK, the ATPase subunit of the trehalose/maltose ABC transporter of the archaeon *Thermococcus litoralis*. *Embo J* 2000;19:5951–5961. [PubMed: 11080142]
35. Zaitseva J, Jenewein S, Oswald C, Jumpertz T, Holland IB, Schmitt L. A molecular understanding of the catalytic cycle of the nucleotide-binding domain of the ABC transporter HlyB. *Biochem Soc Trans* 2005;33:990–995. [PubMed: 16246029]
36. Zaitseva J, Oswald C, Jumpertz T, Jenewein S, Wiedenmann A, Holland IB, Schmitt L. A structural analysis of asymmetry required for catalytic activity of an ABC-ATPase domain dimer. *Embo J* 2006;25:3432–3443. [PubMed: 16858415]
37. Dawson RJ, Hollenstein K, Locher KP. Uptake or extrusion: crystal structures of full ABC transporters suggest a common mechanism. *Mol Microbiol* 2007;65:250–257. [PubMed: 17578454]
38. Hollenstein K, Dawson RJ, Locher KP. Structure and mechanism of ABC transporter proteins. *Curr Opin Struct Biol* 2007;17:412–418. [PubMed: 17723295]
39. Pinkett HW, Lee AT, Lum P, Locher KP, Rees DC. An inward-facing conformation of a putative metal-chelate-type ABC transporter. *Science* 2007;315:373–377. [PubMed: 17158291]
40. Kozak M. Point mutations define a sequence flanking the AUG initiator codon that modulates translation by eukaryotic ribosomes. *Cell* 1986;44:283–292. [PubMed: 3943125]
41. Palmiter RD, Behringer RR, Quaipe CJ, Maxwell F, Maxwell IH, Brinster RL. Cell lineage ablation in transgenic mice by cell-specific expression of a toxin gene. *Cell* 1987;50:435–443. [PubMed: 3649277]*Cell* 1990 Aug 10;62(3):following 608.published erratum appears in

42. Chang XB, Tabcharani JA, Hou YX, Jensen TJ, Kartner N, Alon N, Hanrahan JW, Riordan JR. Protein kinase A (PKA) still activates CFTR chloride channel after mutagenesis of all 10 PKA consensus phosphorylation sites. *J Biol Chem* 1993;268:11304–11311. [PubMed: 7684377]
43. Chang XB, Hou YX, Riordan JR. ATPase activity of purified multidrug resistance-associated protein. *J Biol Chem* 1997;272:30962–30968. [PubMed: 9388243] *J Biol Chem* 1998 Mar 27;273(13):7782. published erratum appears in
44. Hou Y, Cui L, Riordan JR, Chang XB. Allosteric interactions between the two non-equivalent nucleotide binding domains of multidrug resistance protein MRP1. *J Biol Chem* 2000;275:20280–20287. [PubMed: 10781583]
45. Orban TI, Seres L, Ozvegy-Laczka C, Elkind NB, Sarkadi B, Homolya L. Combined localization and real-time functional studies using a GFP-tagged ABCG2 multidrug transporter. *Biochem Biophys Res Commun* 2008;367:667–673. [PubMed: 18182157]
46. Hynes TR, Tang L, Mervine SM, Sabo JL, Yost EA, Devreotes PN, Berlot CH. Visualization of G protein betagamma dimers using bimolecular fluorescence complementation demonstrates roles for both beta and gamma in subcellular targeting. *J Biol Chem* 2004;279:30279–30286. [PubMed: 15136579]
47. Cui L, Hou YX, Riordan JR, Chang XB. Mutations of the Walker B motif in the first nucleotide binding domain of multidrug resistance protein MRP1 prevent conformational maturation. *Arch Biochem Biophys* 2001;392:153–161. [PubMed: 11469806]
48. Leier I, Jedlitschky G, Buchholz U, Keppler D. Characterization of the ATP-dependent leukotriene C4 export carrier in mastocytoma cells. *Eur J Biochem* 1994;220:599–606. [PubMed: 8125120]
49. Loe DW, Almquist KC, Deeley RG, Cole SP. Multidrug resistance protein (MRP)-mediated transport of leukotriene C4 and chemotherapeutic agents in membrane vesicles. Demonstration of glutathione-dependent vincristine transport. *J Biol Chem* 1996;271:9675–9682. [PubMed: 8621643]
50. Robey RW, Honjo Y, van de Laar A, Miyake K, Regis JT, Litman T, Bates SE. A functional assay for detection of the mitoxantrone resistance protein, MXR (ABCG2). *Biochim Biophys Acta* 2001;1512:171–182. [PubMed: 11406094]
51. Mitomo H, Kato R, Ito A, Kasamatsu S, Ikegami Y, Kii I, Kudo A, Kobatake E, Sumino Y, Ishikawa T. A functional study on polymorphism of the ATP-binding cassette transporter ABCG2: critical role of arginine-482 in methotrexate transport. *Biochem J* 2003;373:767–774. [PubMed: 12741957]
52. Ishikawa T, Kasamatsu S, Hagiwara Y, Mitomo H, Kato R, Sumino Y. Expression and functional characterization of human ABC transporter ABCG2 variants in insect cells. *Drug Metab Pharmacokinet* 2003;18:194–202. [PubMed: 15618735]
53. Xu J, Liu Y, Yang Y, Bates S, Zhang JT. Characterization of oligomeric human half-ABC transporter ATP-binding cassette G2. *J Biol Chem* 2004;279:19781–19789. [PubMed: 15001581]
54. Henriksen U, Gether U, Litman T. Effect of Walker A mutation (K86M) on oligomerization and surface targeting of the multidrug resistance transporter ABCG2. *J Cell Sci* 2005;118:1417–1426. [PubMed: 15769853]
55. Volk EL, Schneider E. Wild-type breast cancer resistance protein (BCRP/ABCG2) is a methotrexate polyglutamate transporter. *Cancer Res* 2003;63:5538–5543. [PubMed: 14500392]
56. Chen ZS, Robey RW, Belinsky MG, Shchaveleva I, Ren XQ, Sugimoto Y, Ross DD, Bates SE, Kruh GD. Transport of methotrexate, methotrexate polyglutamates, and 17beta-estradiol 17-(beta-D-glucuronide) by ABCG2: effects of acquired mutations at R482 on methotrexate transport. *Cancer Res* 2003;63:4048–4054. [PubMed: 12874005]
57. Urbatsch IL, Julien M, Carrier I, Rousseau ME, Cayrol R, Gros P. Mutational analysis of conserved carboxylate residues in the nucleotide binding sites of P-glycoprotein. *Biochemistry* 2000;39:14138–14149. [PubMed: 11087362]
58. Payen LF, Gao M, Westlake CJ, Cole SP, Deeley RG. Role of carboxylate residues adjacent to the conserved core Walker B motifs in the catalytic cycle of multidrug resistance protein 1 (ABCC1). *J Biol Chem* 2003;278:38537–38547. [PubMed: 12882957]
59. Yang R, McBride A, Hou YX, Goldberg A, Chang XB. Nucleotide dissociation from NBD1 promotes solute transport by MRP1. *Biochim Biophys Acta* 2005;1668:248–261. [PubMed: 15737336]
60. Robey RW, Obrzut T, Shukla S, Polgar O, Macalou S, Bahr JC, Di Pietro A, Ambudkar SV, Bates SE. Becatecarin (rebeccamycin analog, NSC 655649) is a transport substrate and induces expression

of the ATP-binding cassette transporter, ABCG2, in lung carcinoma cells. *Cancer Chemother Pharmacol.* 2009

61. Ozvegy C, Litman T, Szakacs G, Nagy Z, Bates S, Varadi A, Sarkadi B. Functional characterization of the human multidrug transporter, ABCG2, expressed in insect cells. *Biochem Biophys Res Commun* 2001;285:111–117. [PubMed: 11437380]
62. Mao Q, Conseil G, Gupta A, Cole SP, Unadkat JD. Functional expression of the human breast cancer resistance protein in *Pichia pastoris*. *Biochem Biophys Res Commun* 2004;320:730–737. [PubMed: 15240109]
63. Janvilisri T, Venter H, Shahi S, Reuter G, Balakrishnan L, van Veen HW. Sterol transport by the human breast cancer resistance protein (ABCG2) expressed in *Lactococcus lactis*. *J Biol Chem* 2003;278:20645–20651. [PubMed: 12668685]
64. Bhatia A, Schafer HJ, Hrycyna CA. Oligomerization of the human ABC transporter ABCG2: evaluation of the native protein and chimeric dimers. *Biochemistry* 2005;44:10893–10904. [PubMed: 16086592]
65. McDevitt CA, Crowley E, Hobbs G, Starr KJ, Kerr ID, Callaghan R. Is ATP binding responsible for initiating drug translocation by the multidrug transporter ABCG2? *Febs J* 2008;275:4354–4362. [PubMed: 18657189]
66. Gao M, Cui HR, Loe DW, Grant CE, Almquist KC, Cole SP, Deeley RG. Comparison of the functional characteristics of the nucleotide binding domains of multidrug resistance protein 1. *J Biol Chem* 2000;275:13098–13108. [PubMed: 10777615]
67. Buyse F, Hou YX, Vigano C, Zhao Q, Ruyschaert JM, Chang XB. Replacement of the positively charged Walker A lysine residue with a hydrophobic leucine residue and conformational alterations caused by this mutation in MRP1 impair ATP binding and hydrolysis. *Biochem J* 2006;397:121–130. [PubMed: 16551273]
68. Yang R, Scavetta R, Chang XB. The hydroxyl group of S685 in Walker A motif and the carboxyl group of D792 in Walker B motif of NBD1 play a crucial role for multidrug resistance protein folding and function. *Biochim Biophys Acta* 2008;1778:454–465. [PubMed: 18088596]
69. Payen L, Gao M, Westlake C, Theis A, Cole SP, Deeley RG. Functional Interactions Between Nucleotide Binding Domains and Leukotriene C4 Binding Sites of Multidrug Resistance Protein 1 (ABCC1). *Mol Pharmacol* 2005;67:1944–1953. [PubMed: 15755910]

### The abbreviations used are

<b>ABCG2</b>	ATP binding cassette group G2
<b>P-gp</b>	P-glycoprotein
<b>MRP1</b>	multidrug resistance protein
<b>CFTR</b>	cystic fibrosis transmembrane-conductance regulator
<b>NBD</b>	nucleotide binding domain
<b>EDTA</b>	ethylenediaminetetraacetic acid
<b>EGTA</b>	ethylene glycol-bis( $\beta$ -aminoethyl ether)N,N,N,N-tetraacetic acid
<b>SDS</b>	sodium dodecyl sulfate

<b>MTX</b>	methotrexate
<b><math>\beta</math>-ME</b>	$\beta$ -mercaptoethanol
<b>DTT</b>	dithiothreitol
<b>BHK</b>	baby hamster kidney
<b>LTC4</b>	leukotriene C4

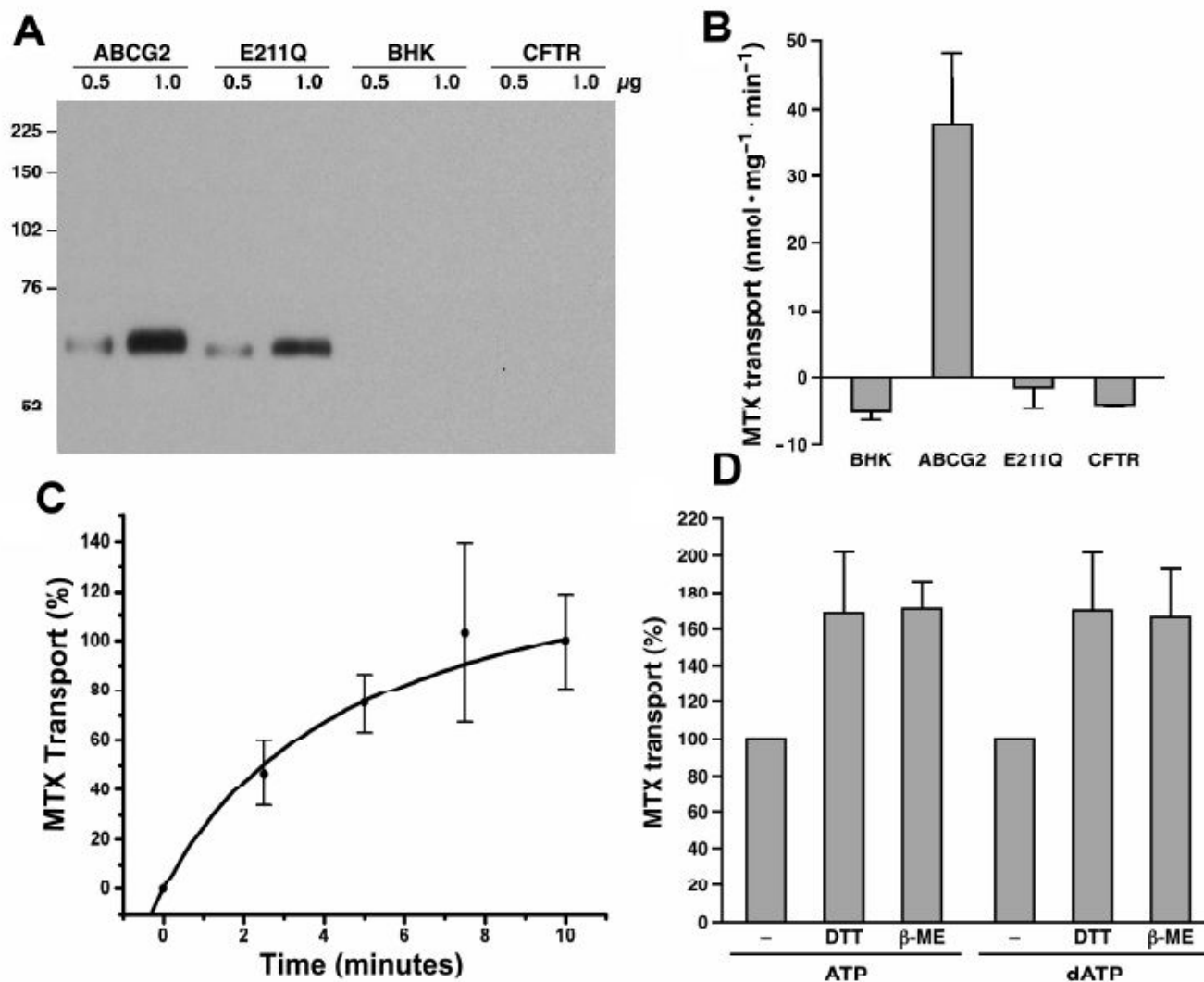


**Figure 1.**

Substitution of the putative catalytic base E211 with a non-acidic amino acid Q completely abolished its ATP-dependent MTX transport. A. Expression of wt and E211Q-mutated ABCG2 in BHK cells. Membrane proteins (0.5 and 1 µg) were subjected to SDS-PAGE (7%), electroblotted to a nitrocellulose membrane and probed with ABCG2-specific monoclonal antibody BXP-21. Molecular weight markers are indicated on the left. B. E211Q-mutated ABCG2 is unable to transport MTX into the membrane vesicles. The dATP (4 mM) dependent MTX transport by ABCG2, E211Q, BHK or CFTR membrane vesicles was performed in triplicate according to the method described in Experimental Procedures. The amount of MTX bound to the membrane vesicles in the presence of 4 mM AMP was subtracted from the MTX accumulated in the presence of 4 mM dATP. C. Time-dependent MTX transport. The time-dependent MTX transport was performed (in triplicate) in the presence of 3 µg of ABCG2 membrane vesicles and 4 mM dATP. The amount of MTX accumulated in the membrane vesicles within 10 minutes at 37 °C was considered as 100%. D. Reducing agents enhanced the nucleotide dependent MTX transport. The experiments were performed in the absence or presence of 10 mM dithiothreitol (DTT) or 10 mM β-mercaptoethanol (β-ME).

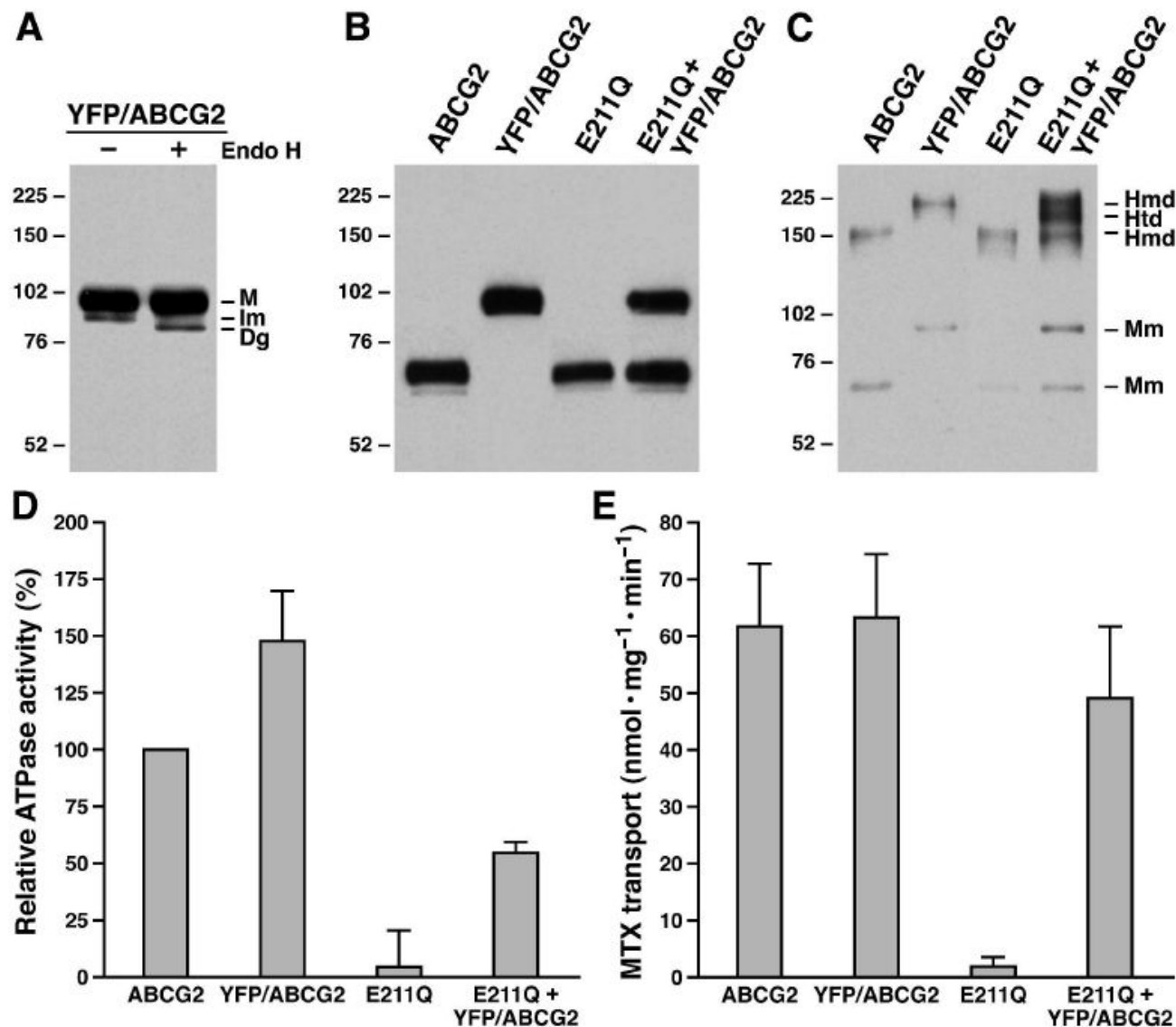


**Figure 2.** Heterodimer of YFP/ABCG2 and E211Q-mutated ABCG2 may be able to transport MTX across the biological membranes. **A.** YFP/ABCG2 fusion protein mainly forms complex-glycosylated protein at 37 °C. Membrane vesicles containing YFP/ABCG2 fusion protein was digested with endoglycosidase H according to the method described in Experimental Procedures. M, Im and Dg on the right indicate the mature, the core-glycosylated immature and the deglycosylated YFP/ABCG2. **B.** The relative amounts of ABCG2 proteins in membrane vesicles. Membrane vesicles (1 µg) containing wt ABCG2, YFP/ABCG2, E211Q or YFP/ABCG2 + E211Q were subjected to SDS-PAGE (7%) and probed with ABCG2 mAb BXP-21. The intensities of the ABCG2 protein bands were measured by a scanning densitometer and used to determine the ratios between them. **C.** Co-expression of YFP/ABCG2 and E211Q in BHK cells forms homodimers and heterodimer. Membrane vesicles containing wt ABCG2 (0.5 µg), YFP/ABCG2 (0.5 µg), E211Q (0.5 µg) or YFP/ABCG2 + E211Q (1 µg) were subjected to SDS-PAGE (4-10% gradient gel) in the absence of reducing agent DTT and probed with ABCG2 mAb BXP-21. The intensities of the ABCG2 protein bands were measured

by a scanning densitometer and used to determine the ratios between them. Molecular weight markers are indicated on the left. Mm, Hmd and Htd on the right indicate the monomers of ABCG2, E211Q or YFP/ABCG2, the homodimers of ABCG2, E211Q or YFP/ABCG2 and the heterodimer of YFP/ABCG2 and E211Q. D. E211Q-mutated ABCG2 is unable to hydrolyze ATP. The ATPase assay (in triplicate) was performed according to the method described in Experimental Procedures by using 2  $\mu\text{g}$  of the same membrane vesicles shown in Figure 2B and 2C (1.8862  $\mu\text{g}$  of wtABCG2 + 0.1138  $\mu\text{g}$  of BHK; 1.5145  $\mu\text{g}$  of YFP/ABCG2 + 0.4855  $\mu\text{g}$  of BHK; 2  $\mu\text{g}$  of E211Q; and 0.7918  $\mu\text{g}$  of YFP/ABCG2 + E211Q + 1.2082  $\mu\text{g}$  of BHK) and 4 mM ATP at 37 °C for 30 minutes. After subtraction of the amount of inorganic phosphate generated in the presence of 2  $\mu\text{g}$  BHK membrane vesicles, the velocity of the ATPase activity was calculated and compared to that of ABCG2 (n = 5). E. The heterodimer of YFP/ABCG2 and E211Q may be able to transport MTX across the biological membranes. The MTX uptake assays were carried out, according to the method described in Experimental Procedures, in a 30  $\mu\text{l}$  solution (in triplicate) containing 3  $\mu\text{g}$  of membrane vesicles (2.829  $\mu\text{g}$  of ABCG2 + 0.171  $\mu\text{g}$  of BHK; 2.272  $\mu\text{g}$  of YFP/ABCG2 + 0.728  $\mu\text{g}$  of BHK; 3  $\mu\text{g}$  of E211Q; and 1.188  $\mu\text{g}$  of YFP/ABCG2 + E211Q + 1.812  $\mu\text{g}$  of BHK), 2 mM MTX, 10 mM DTT and 4 mM dATP at 37 °C for 7.5 minutes. After subtraction of the amount of radioactivity bound to the nitrocellulose membrane in the presence of 4 mM AMP from the same sample in the presence of 4 mM dATP, the velocity of the dATP-dependent MTX transport was calculated (n = 4).



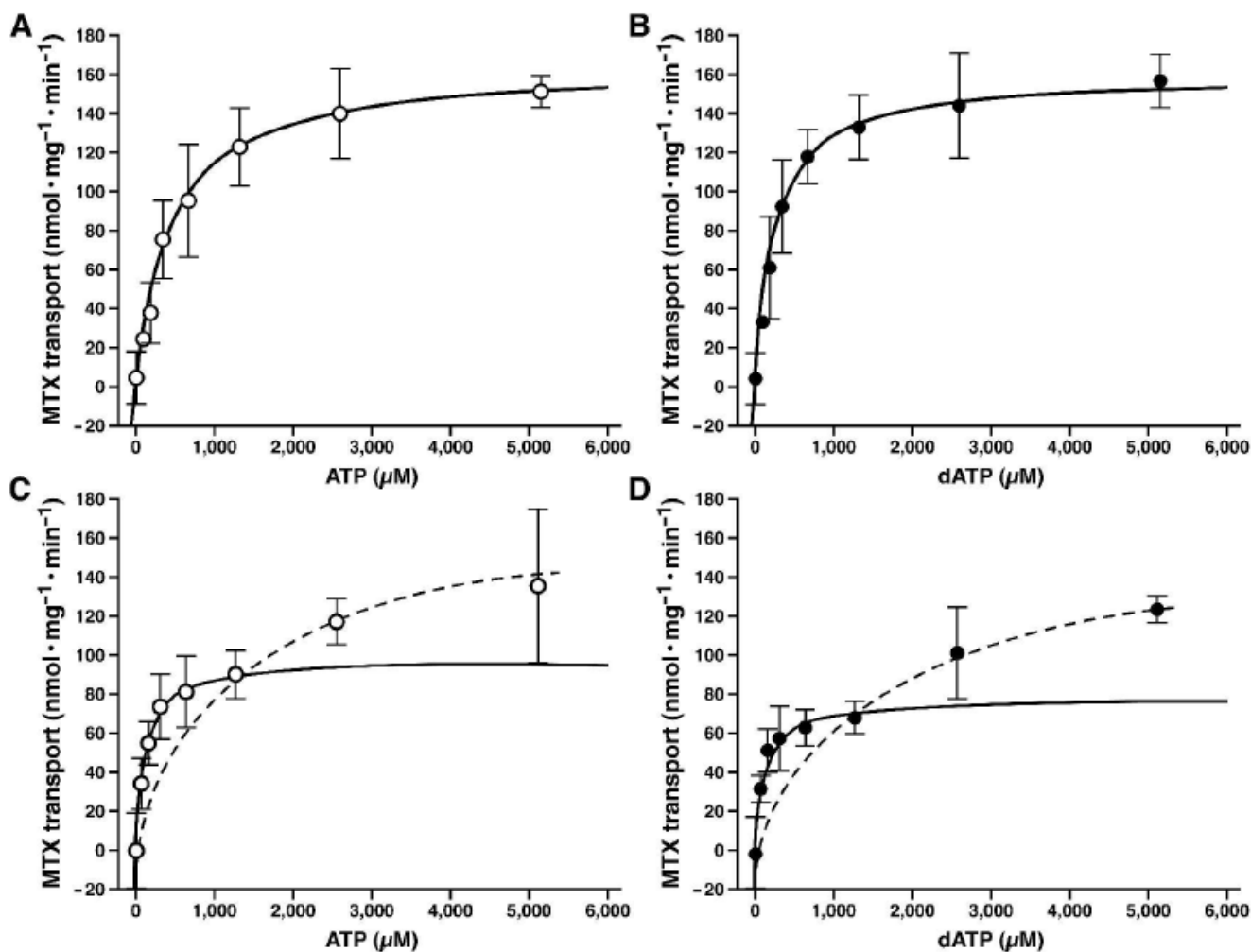


**Figure 3.**

Insertion of YFP protein into the N-terminus of ABCG2 did not significantly affect its nucleotide-dependent MTX transport. The MTX uptake assays were carried out, according to the method described in Experimental Procedures, in triplicate with 3 μg of membrane vesicles shown in Figure 2B and 2C in the presence of varying concentrations of ATP or dATP and 10 mM DTT. A. ATP-dependent MTX transport by YFP/ABCG2. B. dATP-dependent MTX transport by YFP/ABCG2. C. ATP-dependent MTX transport by YFP/ABCG2 + E211Q. D. dATP-dependent MTX transport by YFP/ABCG2 + E211Q.

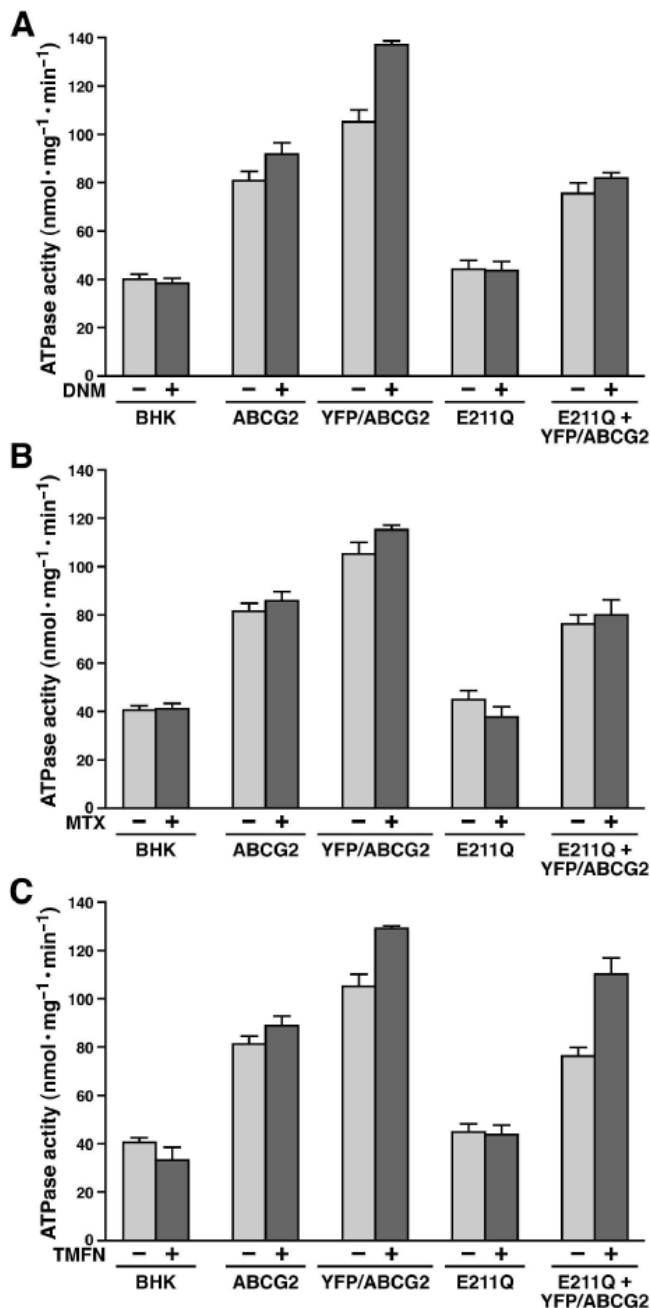


**Figure 4.**

Drug effects on the ATPase activities of ABCG2 proteins. The ATPase assay (in triplicate) was performed according to the method described in Experimental Procedures by using  $2 \mu\text{g}$  of each sample shown in Figure 2B and 2C and  $4 \text{ mM}$  ATP in the absence (-) or presence (+) of  $100 \mu\text{M}$  daunomycin (DNM) (A),  $1 \text{ mM}$  methotrexate (MTX) (B) or  $200 \mu\text{M}$  tamoxifen citrate (TMXF) (C) at  $37^\circ\text{C}$  for 30 minutes. After subtraction of the amount of inorganic phosphate generated in the presence of  $4 \text{ mM}$  ATP (without any membrane vesicles), the velocity of the ATPase activity was calculated ( $n = 4$ ).

**Table 1**Relative MTX transport activity<sup>a</sup>

Sample	MTX transport (%)
ABCG2	100.0 ± 0.0
YFP/ABCG2	101.2 ± 2.4
E211Q	3.7 ± 3.3
YFP/ABCG2+E211Q	79.4 ± 11.2

<sup>a</sup>The data were derived from Figure 2E (n=4).

**Table 2** $K_m$  and  $V_{max}$  values of wt and mutant ABCG2

Sample	$K_m$ ( $\mu$ M ATP)	ATP $V_{max}$ (nmol/mg/min)	$K_m$ ( $\mu$ M dATP)	dATP $V_{max}$ (nmol/mg/min)
ABCG2	424.4 $\pm$ 22.4	143.7 $\pm$ 1.7	251.3 $\pm$ 13.0	131.4 $\pm$ 5.4
YFP/ABCG2	455.0 $\pm$ 18.7	160.7 $\pm$ 21.3	274.2 $\pm$ 31.4	149.2 $\pm$ 9.9
YFP/ABCG2+E211Q	?	?	?	?